PERFUSION AND DIFFUSION TENSOR IMAGING IN A PATIENT WITH LOCKED-IN SYNDROME AFTER NEUROSURGICAL VASCULAR BYPASS AND ENDOVASCULAR EMBOLIZATION OF A BASILAR ARTERY ANEURYSM: CASE REPORT

Yvonne W. Lui, M.D.
Department of Radiology,
New York University
Medical Center,
New York, New York

Meng Law, M.D.
Departments of Radiology
and Neurosurgery,
New York University
Medical Center,
New York, New York

Jafar J. Jafar, M.D.
Department of Neurosurgery,
New York University
Medical Center,
New York, New York

Andrea Douglas, M.D.
Department of Neurosurgery,
New York University
Medical Center,
New York, New York

Peter Kim Nelson, M.D.
Department of Radiology,
New York University
Medical Center,
New York, New York

Reprint requests:
Yvonne W. Lui, M.D.,
NYU Medical Center,
Department of Radiology,
Section of Neuroradiology,
530 First Avenue,
New York, NY 10016.
Email: luiy01@med.nyu.edu

Received, June 17, 2005.
Accepted, November 19, 2005.

OBJECTIVE AND IMPORTANCE: Locked-in syndrome is a state of preserved consciousness in the setting of quadriplegia, anarthria, and usually also includes lateral gaze palsy. It is most commonly associated with upper brainstem infarction variably sparing the third cranial nerve nucleus. There are likely many etiologies that contribute to this clinical syndrome. These are incompletely understood, and the syndrome remains a rare but devastating complication that can occur after neurosurgical and neurovascular interventions. Advanced magnetic resonance imaging techniques such as perfusion and diffusion tensor imaging may help to elucidate the mechanism behind locked-in syndrome. To the authors' knowledge, there are no reports in the literature of perfusion and diffusion tensor findings in patients with this syndrome. A postprocedural case of locked-in syndrome is described with abnormalities on perfusion and diffusion tensor imaging in the absence of any changes in conventional magnetic resonance imaging.

CLINICAL PRESENTATION: A 57-year-old man who presented with acute onset headache, ataxia, and other nonspecific symptoms was found on imaging to have a giant fusiform basilar artery aneurysm.

INTERVENTION: A saphenous vein graft bypass between the proximal right external carotid artery and P2 segment of the right posterior cerebral artery followed immediately by endovascular embolization of the aneurysm sac and distal left vertebral artery was performed.

CONCLUSION: Postprocedural angiography demonstrated patency of the bypass graft, and diffusion weighted imaging showed no evidence for acute brainstem infarction. Nevertheless, despite technically successful procedures and the absence of abnormalities on conventional magnetic resonance imaging, the patient developed quadriplegia and anarthria and remained in a locked-in state until he expired. Abnormalities were, however, seen on both perfusion and diffusion tensor imaging, where hypoperfusion, increased mean diffusivity, and decreased fractional anisotropy were observed in the ventral brainstem. The findings suggested a disruption of pontine white matter tracts. Advanced imaging techniques may allow us to image important microstructural changes that were previously not discernable and assist in the evaluation of patients with complex neurological sequelae such as locked-in syndrome.

KEY WORDS: Basilar artery aneurysm, Diffusion tensor imaging, Locked-in syndrome, Perfusion

Neurosurgery 58:794-795, 2006 DOI: 10.1227/01.NEU.0000204893.07192.1F www.neurosurgery-online.com

Locked-in syndrome, a term coined by Plum and Posner (11) in 1966, is a clinical diagnosis made by the presence of upper motor neuron quadriplegia and lower cranial nerve dysfunction most commonly with preservation of the oculomotor nucleus that leaves the patient conscious and able to communicate only via blinking and most frequently preserves vertical movements of the eyes. The most common etiology is stroke, with 75 to 85% of cases attributable to upper brainstem infarction (5, 9). Other etiologies include pontine hemorrhage, trauma (5), tumor (6), central pontine myelinolysis (10), and infection (7). It

has been described as a rare complication of surgery in which the underlying etiology was also most frequently ischemic (1).

Despite new surgical and endovascular techniques, giant fusiform basilar artery aneurysms present a therapeutic challenge because of their location at the cranial base, adjacent to critical brainstem structures (2). We describe diffusion tensor and perfusion magnetic resonance imaging (MRI) findings in a case of locked-in syndrome after neurovascular bypass and embolization of a giant basilar artery aneurysm and discuss the potential role of advanced MRI techniques in the evaluation of such patients.

CASE REPORT

Clinical History

A 57-year-old man with past medical history of peripheral neuropathy, presumptively diagnosed as Charcot Marie Tooth Syndrome, was referred for treatment of a giant fusiform aneurysm of the proximal basilar artery. Three months earlier, he was hospitalized with acute onset of crushing headache accompanied by dizziness, unsteady gait, blurred vision, and nausea. The diagnostic workup, including head computed tomography, brain MRI, intracranial computed tomographic angiography, and conventional cerebral angiography, was significant for a partially thrombosed giant fusiform aneurysm with evidence of acute intramural hemorrhage involving the distal left vertebral, vertebrobasilar junction, and basilar artery proximal to the anterior inferior cerebellar artery segment. There was considerable mass effect on the ventral pons and medulla (*Fig. 1*). His diplopia and ataxia gradually resolved; however, he continued to experience severe headaches daily, and, on admission for treatment, his neurological examination was significant for spastic myelopathy and unsteady gait. After consideration of the risks and benefits of surgical and neurointerventional therapies versus conservative management, the patient was admitted for combined surgical/endovascular treatment and subsequently underwent surgical establishment of a saphenous vein graft bypass between the proximal right external carotid artery and P2 segment of the right posterior cerebral artery followed immediately by endovascular occlusion of the aneurysm sac and distal left vertebral artery with combination Guglielmi detachable and platinum fiber coils. Posttreatment angiography demonstrated occlusion of the aneurysm with collateral reconstitution of the distal basilar artery and anterior inferior cerebellar arteries through the surgical graft (*Fig. 2*).

Although able to move all extremities to command after his emergence from generalized anesthesia, within 4 hours, the patient became unresponsive with a flaccid quadriparesis. Over the next 2 hours, his neurological examination evolved with recovery of bilateral eye opening and an improved level of consciousness with brisk responses to yes and no questions via eye-blinking. His examination, however, was otherwise significant for a left lateral gaze preference, decerebrate posturing to noxious stimuli, and the inability to voluntarily move his head or mouth.

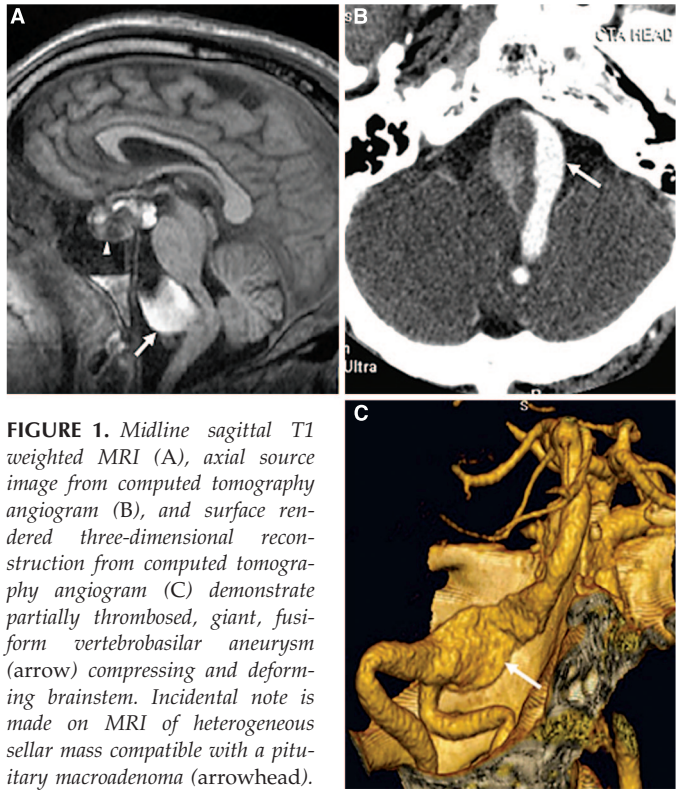

FIGURE 1. *Midline sagittal T1 weighted MRI (*A*), axial source image from computed tomography angiogram (*B*), and surface rendered three-dimensional reconstruction from computed tomography angiogram (*C*) demonstrate partially thrombosed, giant, fusiform vertebrobasilar aneurysm (*arrow*) compressing and deforming brainstem. Incidental note is made on MRI of heterogeneous sellar mass compatible with a pituitary macroadenoma (*arrowhead*).*

FIGURE 2. *Images from postprocedure digital subtraction angiogram.* A, *selected injection into right vertebral artery demonstrates opacification of anterior spinal artery (*black arrow*) and right posterior inferior cerebellar artery (*black arrowhead*). Subtraction artifact from coil mass seen within thrombosed aneurysm.* B, *selected injection into bypass graft demonstrates patency of graph (*arrowhead*) with good opacification of posterior cerebral arteries and retrograde flow into distal basilar artery. Left anterior inferior cerebellar artery is well demonstrated (*white arrow*).*

Conventional postoperative MRI demonstrated no brainstem infarction. Brainstem auditory evoked potentials were performed and were normal; however, somatosensory evoked potentials, and motor evoked potentials were absent. Over the following weeks, his examination gradually deteriorated. MRI, brainstem auditory evoked potentials, somatosensory evoked potentials, and motor evoked potentials were repeated

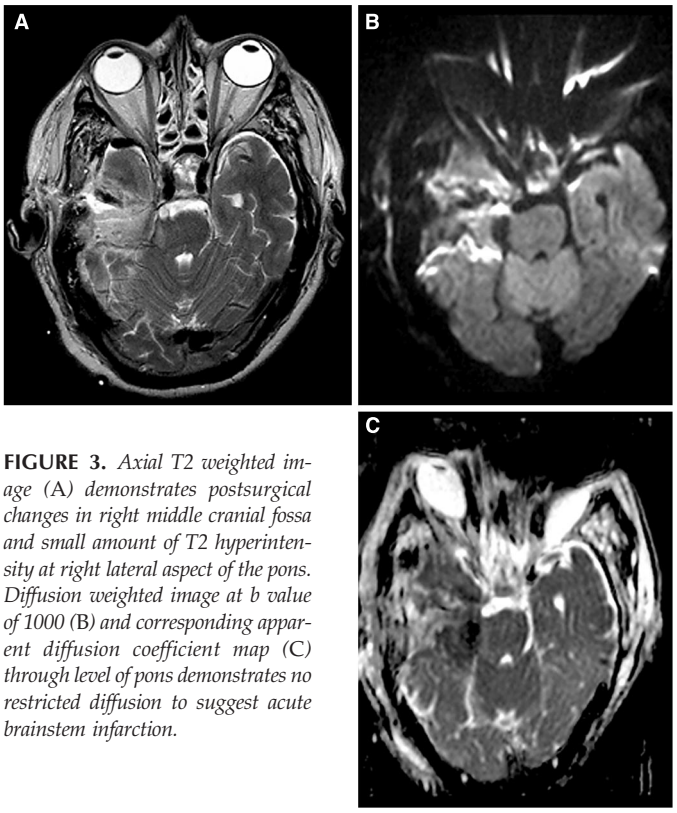

FIGURE 3. *Axial T2 weighted image (A) demonstrates postsurgical changes in right middle cranial fossa and small amount of T2 hyperintensity at right lateral aspect of the pons. Diffusion weighted image at b value of 1000 (B) and corresponding apparent diffusion coefficient map (C) through level of pons demonstrates no restricted diffusion to suggest acute brainstem infarction.*

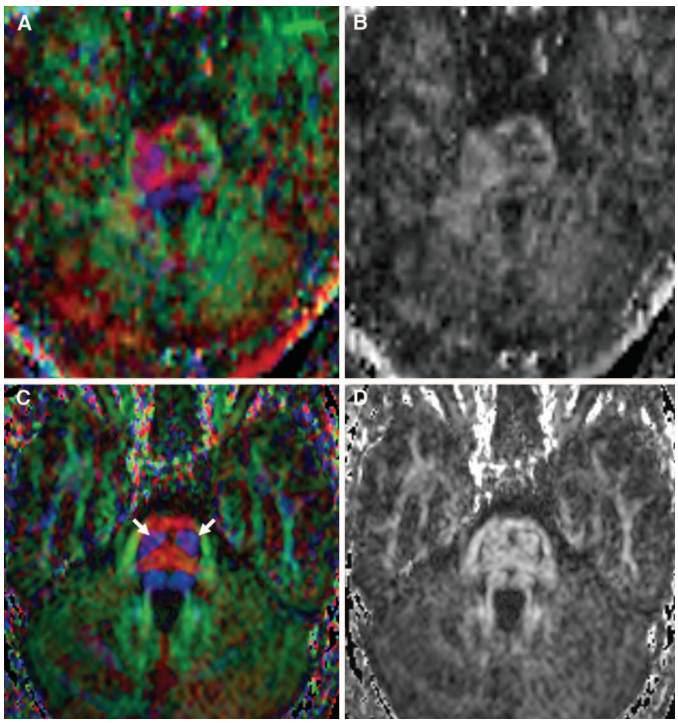

FIGURE 4. A and B, *fractional anisotropy directional color map (A) and fractional anisotropy map (B) demonstrating poor visualization of corticospinal tracts at level of mid pons. There is decreased FA and increased mean diffusivity in brainstem, more on B side than A. C and D, normal control is provided for comparison, demonstrating corticospinal tracts encoded blue in superior-inferior direction in anterior pons (arrows).*

and were unchanged in comparison with the initial evaluation.

After 4 weeks, the patient was returned to the operating room for resection of the aneurysm sac in an effort to relieve presumptive brainstem compression. The patient tolerated this procedure well but remained locked-in with no change in evoked potentials and expired approximately 6 weeks after his initial procedure.

MRI

On postprocedure day 1, MRI was performed on a 1.5 Tesla system (Siemens Sonata or Symphony, Siemens AG, Erlangen, Germany). A localizing sagittal T1-weighted image was obtained followed by nonenhanced axial T1-weighted spin echo (repetition time/echo time, 600/14 ms), axial fluid-attenuated inversion recovery (fluid attenuated inversion recovery, 9000/110/inversion time 2500), and T2-weighted (3400/119) images). Diffusion weighted imaging and diffusion tensor imaging were also performed.

Conventional MRIs demonstrated expected postoperative and postprocedural changes. There remained mass effect on the brainstem from the aneurysm sac. Diffusion weighted images acquired in the axial plane using an echo-planar imaging sequence with b values of 0, 500, and 1000 seconds mm^{-2} demonstrated no restricted diffusion within the brainstem to suggest acute infarction (*Fig. 3*).

Diffusion tensor imaging using echo planar technique imaging (repetition time/echo time, 5300/74; 128 $\times$ 128 matrix; 220 $\times$ 220 mm field of view; 45 3 mm contiguous slices; b = 1000 s/mm^2) was also performed using six gradient directions. Mean diffusivity, fractional anisotropy (FA), and color-coded direction of maximum anisotropy maps were then generated. There was an abnormal appearance to the brainstem white matter tracts. In particular, at the level of the mid pons, the corticospinal tracts were poorly visualized on the FA color maps (*Fig. 4*) and region of interest FA measures in the corticospinal tracts were low, measuring 0.526 and 0.343, respectively, on the right and left at the level of the pons. The corresponding mean diffusivity measures at this level were high, measuring 0.888 and 1.478 (*Table 1*). Seed areas placed in the expected location of the corticospinal tracts at the level of the mid pons demonstrated decreased number and extent of fiber tracts (*Fig. 5*) compared with a normal control.

Follow-up MRI 3 days later showed no change on conventional images. Once again, there was no restricted diffusion in the brainstem. Perfusion imaging using dynamic susceptibility contrast MRI was performed and showed diminished cerebral blood flow, cerebral blood volume, and prolonged mean transit time in the brainstem, particularly in the pons and medulla (*Table 1*) (*Fig. 6*). Diffusion tensor imaging was repeated as well on postproce-

TABLE 1. Brainstem diffusion tensor and perfusion metrics in a patient with locked-in syndrome[a]

		DTI		DSC MRI		
Location		**FA**	**MD**	**CBF**	**CBV**	**MTT**
Midbrain	R	0.529 (0.774)	0.71 (0.861)	9.3 (43.3)	0.48 (2.01)	3.11 (2.79)
	L	0.778 (0.747)	0.639 (.753)	14.1 (44.2)	0.73 (2.26)	3.11 (3.07)
Pons	R	0.526 (0.588)	0.888 (0.715)	17.5 (42.5)	0.99 (2.25)	3.4 (3.17)
	L	0.343 (0.606)	1.478 (0.858)	10.8 (36.3)	0.58 (1.93)	3.22 (3.18)
Medulla [b]	R	0.320 (0.455)	0.875 (1.216)	16.9 (46.7)	1.02 (1.90)	3.63 (3.13)
	L	0.366 (0.508)	0.799 (1.053)			

[a] DTI, diffusion tensor imaging; DSC MRI, dynamic susceptibility contrast perfusion magnetic resonance imaging; FA, fractional anisotropy; MD, mean diffusivity, these measures were taken in the region of the corticospinal tracts at the levels noted; CBF, cerebral blood flow (ml/100g/min); CBV, cerebral blood volume (ml/100g); MTT, mean transit time(s); R, right; L, left. Numbers in parentheses indicate normal values from an age/sex match control.
[b] Data obtained in the lower brainstem may not be as reliable because of susceptibility artifact. Perfusion data in the medulla were obtained from a region of interest placed in the midline.

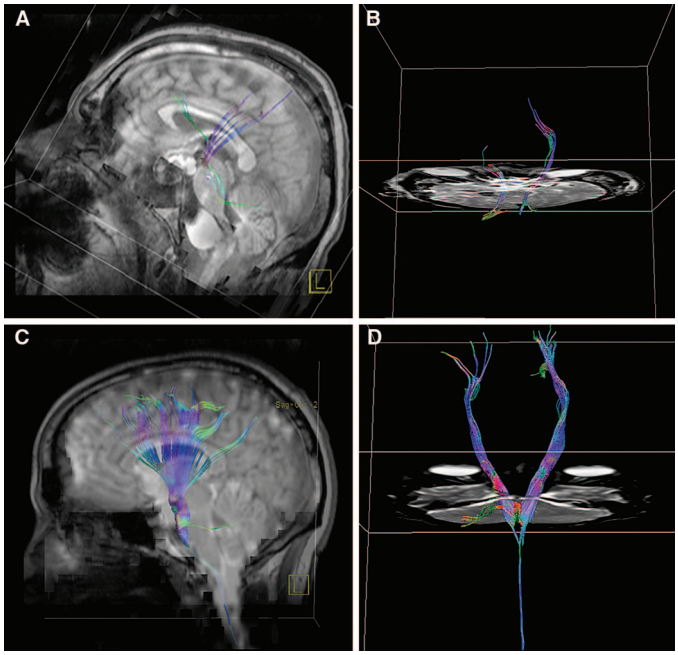

FIGURE 5. A, *tractography sagittal projection* (A) *superimposed on corresponding sagittal T1 weighted image and three-dimensional anterior-posterior projection* (B) *with seeds placed within expected location of corticospinal tracts bilaterally in mid pons. Sagittal projection demonstrates relationship of fiber tracts to aneurysm with no fibers tracked inferior to mid pontine level.* C and D, *normal control is provided for comparison, demonstrating normal number and course of corticospinal tracts.*

dure day 4. There was no change in the FA measures within the corticospinal tracts or in the overall appearance of the FA color maps and tractography.

DISCUSSION

Despite the postoperative development of a clinically apparent locked-in state in our patient, supported by disruptions in motor and somatosensory evoked potentials, conventional spin-echo and diffusion MRI sequences were noncontributory, failing to confirm the anticipated brainstem stroke. Perfusion and diffusion tensor imaging, however, demonstrated clear abnormalities within the brainstem. This suggests that advanced MRI techniques can detect critical microstructural changes that are not visible on conventional MRIs.

In our patient, the diffusion tensor metrics and MRI tractography suggested a profound disruption of ventral fibers at the pontomesencephalic junction, which corresponded to the clinical manifestations evident on neurological examination. The etiology of this disruption, unfortunately, is less clear. Two possible mechanisms might include chronic subinfarct brainstem ischemia versus a critical exacerbation of aneurysmal mass effect.

In terms of brainstem ischemia, imaging obtained during the course of the patient's hospitalization is conflicted. Angiography repeated 2 weeks after symptom onset confirmed maintained bypass support of the distal basilar artery and anterior inferior cerebellar arteries and diffusion weighted imaging showed no acute brainstem infarction. On the other hand, MRI perfusion demonstrated a slight prolongation in the mean transit time with decreased blood flow and decreased blood volume compared with published data from normal subjects (3). Global brainstem vascular compromise may have been present because of a number of different reasons: 1) insufficient arterial collaterals, 2) a transient critical thrombotic event involving the distal basilar artery, the vascular stigmata of which resolved by the time of subsequent angiographic imaging, 3) the effect of acute venous congestion, 4) local vascular insufficiency related to worsening brainstem compression, perhaps related to brief upward herniation, or 5) injury or thrombosis of small basilar arterial perforators.

Of note, it is possible that hypoperfusion as demonstrated by perfusion MRI may have been present before intervention and be a result of longstanding mass effect within the poste-

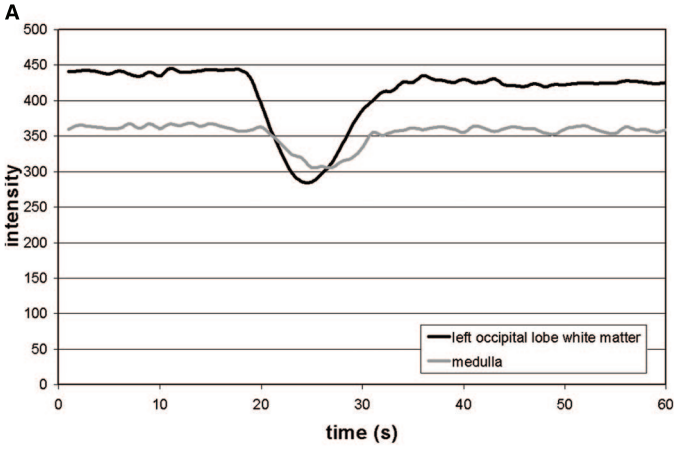

FIGURE 6. A, *dynamic susceptibility contrast perfusion MRI signal intensity curves show diminished perfusion to brainstem in comparison with supratentorial white matter (region of interest placed in left occipital white matter).* B, *cerebral blood volume (CBV) map demonstrates decreased perfusion within brainstem (see also* Table 1*).*

rior fossa. Unfortunately, preoperative baseline perfusion values for the patient were not available for comparison.

Alternatively, critical mass effect on the brainstem without ischemia may have contributed to this patient's clinical decline. A transient or sustained compressive event related to the aneurysmal mass effect could be postulated to result in mechanical disruption of brainstem white matter tracts as supported by the low FA in the corticospinal tracts. Recent work using diffusion tensor imaging has demonstrated that in the normal control, brainstem white matter tracts can be visualized on FA color maps as well as using tractography as robust bilateral tracts running in a superior-inferior direction within the ventral pons (8, 12). We have been able to reproduce this in normal controls at our institution. The exact pathological correlate and clinical significance of abnormal or poorly visualized tracts are unclear. Axonal disruption and white matter edema are among the mechanisms that have been suggested (4).

In view of the potential reversibility of symptoms attributable to persistent mass effect, a decision was made to surgically resect the thrombosed aneurysm sac through a midline posterior suboccipital craniotomy to correct any possible brainstem compressive effect. Although the surgery was technically successful, the patient's clinical status did not improve. Further follow-up imaging continued to demonstrate no brainstem infarction. Repeat diffusion tensor imaging was not interpretable because of susceptibility artifact from surgical hardware relating to the craniotomy.

In this vein, a potential limitation of our report is the fact that minor susceptibility effects attributed to the endovascular coils theoretically could have affected the tractography and tensor metrics obtained during the initial imaging of our patient. We believe that the diffusion tensor imaging performed is reliable as tensor metrics, and tractography of the transverse pontine fibers adjacent to the corticospinal tracts at the same brainstem level were preserved.

The overall prognosis of locked-in syndrome caused by basilar artery occlusion is poor, with clinical recovery occurring rarely, particularly when a vascular etiology is implicated. For patients with locked-in syndrome, conventional CT and MRI are instrumental in determining the presence and extent of brainstem infarction; however, as demonstrated by this case (which was diagnostically confounded by the absence of brainstem diffusion abnormalities as well as the clinical history of Charcot Marie Tooth Syndrome), perfusion and diffusion tensor imaging may have an additional role in confirming an anatomic substrate for the suspected clinical phenomenon and clarifying the pathogenesis and prognosis of patients with cryptic forms of locked-in syndrome.

REFERENCES

1. Breen P, Hannon V: Locked-in syndrome: A catastrophic complication after surgery. **Br J Anaesth** 92:286–288, 2004.
2. Drake CG, Peerless SJ: Giant fusiform intracranial aneurysms: Review of 120 patients treated surgically from 1965 to 1992. **J Neurosurg** 87:141–162, 1997.
3. Helenius J, Perkio J, Soinne L, Ostergaard L, Carano RA, Salonen O, Savolainen S, Kaste M, Aronen HJ, Tatlisumak T: Cerebral hemodynamics in a healthy population measured by dynamic susceptibility contrast MR imaging. **Acta Radiol** 44:538–546, 2003.
4. Jellison BJ, Field AS, Medow J, Lazar M, Salamat MS, Alexander AL: Diffusion tensor imaging of cerebral white matter: A pictorial review of physics, fiber tract anatomy, and tumor imaging patterns. **AJNR Am J Neuroradiol** 25:356–369, 2004.
5. Leon-Carrion J, van Eeckhout P, Dominguez-Morales MR, Perez-Santamaria FJ: The locked-in syndrome: A syndrome looking for a therapy. **Brain Inj** 16:571–582,2002.
6. Masuzawa H, Sato J, Kamitani H, Kamikura T, Aoki N: Pontine gliomas causing locked-in syndrome. **Childs Nerv Syst** 9:256–259, 1993.
7. Murphy MJ, Brenton DW, Aschenbrener CA, Van Gilder JC: Locked-in syndrome caused by a solitary pontine abscess. **J Neurol Neurosurg Psychiatry** 42:1062–1065, 1979.
8. Nagae-Poetscher LM, Jiang H, Wakana S, Golay X, van Zijl PC, Mori S: High-resolution diffusion tensor imaging of the brain stem at 3 T. **AJNR Am J Neuroradiol** 25:1325–1330, 2004.
9. Patterson JR, Grabois M: Locked-in syndrome: A review of 139 cases. **Stroke** 17:758–764, 1986.
10. Pirzada NA, Ali II: Central pontine myelinolysis. **Mayo Clin Proc** 76:559–562, 2001.
11. Plum F, Posner JB: *The Diagnosis of Stupor and Coma.* Philadelphia, F. A. Davis Co., 1966.
12. Stieltjes B, Kaufmann WE, van Zijl PC, Fredericksen K, Pearlson GD, Solaiyappan M, Mori S: Diffusion tensor imaging and axonal tracking in the human brainstem. **Neuroimage** 14:723–735, 2001.

COMMENTS

The authors describe a patient harboring a difficult fusiform posterior circulation aneurysm that developed a post-procedure, locked-in syndrome following revascularization and aneurysm/parent vessel occlusion. Traditional magnetic resonance imaging (MRI) did not fully explain the patient's neurological condition, although perfusion and diffusion tensor imaging demonstrated clear abnormalities in the brainstem.

Fusiform aneurysms of the posterior circulation resulting in brainstem compression unfortunately remain formidable lesions to treat.

The neuroanatomical basis for a locked-in syndrome remains elusive and may be multifactorial. The fact that perfusion and diffusion tensor imaging may identify anatomical abnormalities not delineated by conventional magnetic resonance sequences is interesting. The relative contributions of true ischemic versus non-ischemic events to fiber disruption is meritorious of further study.

The authors have highlighted the potential importance of advanced imaging techniques to help explain clinical symptomatology when conventional methods falter and have highlighted the need for future investigation in this area.

Aaron S. Dumont
Sagi Harnof
Neal F. Kassell
Charlottesville, Virginia

In this case report, the authors describe a 57-year-old male who developed a locked-in syndrome after treatment of a basilar artery aneurysm. Conventional MRI techniques were not helpful in explaining the clinical condition. By contrast, imaging abnormalities were seen on perfusion and diffusion tensor imaging. These techniques can be used to examine white matter structure and help understand anatomic organization and neural connection in human brain. This case report illustrates how advanced neuro-imaging can be applied to clinical problems. The authors are encouraged to pursue these studies in a larger series.

Peter D. Le Roux
Philadelphia, Pennsylvania

In this article, the authors describe a case report of a "locked-in" patient after an attempt to treat a fusiform basilar aneurysm. During this period, multiple diagnostic studies were undertaken and MRI findings, including diffusion tensor imaging and perfusion abnormalities, are described. The paper primarily expresses three major points. One is that we continue to have great difficulty in effectively treating these giant fusiform basilar aneurysms with compression of the brainstem. Multiple theories have been espoused and consistent success is not achieved. In this case, the authors make two attempts to decrease mass effect but still had progressive fatal dysfunction of the brainstem. Second, the syndrome of "locked-in" described by Plum and Posner (1), may have multiple etiologies. In this case, the authors suggest that straightforward ischemia may be augmented by the presence of mass effect or axonal dysfunction. Finally, the authors show magnetic resonance perfusion and diffusion tensor imaging to suggest that there is a differential, at least in this patient, between true infarct and axonal disruption.

The authors emphasize the finding of disruption of white matter tracks without diffusion weighted imaging evidence for acute infarction. Such findings would suggest that the multiple etiologies may lead to the same clinical syndrome. This should encourage clinicians to attempt to define new treatments for those components that may be reversible.

Robert J. Dempsey
Madison, Wisconsin

---

1. Plum F, Posner JB: *The Diagnosis of Stupor and Coma.* Philadelphia, F. A. Davis Co., 1966, ed 2, p 24.